Archives of Hydro-Engineering and Environmental Mechanics
Vol. 45 (1998), No. 1–4, pp. 77–100

Contact Load Model and Sediment Transport Due to Waves Versus Laboratory Data

Leszek M. Kaczmarek, Rafał Ostrowski

Institute of Hydro-Engineering of the Polish Academy of Sciences, ul. Kościerska 7, 80–952 Gdańsk, Poland

(Received September 18, 1998; revised November 26, 1998)

Abstract

A contact load layer model is presented, dealing with the effect of suspended sediment on total sediment transport near the bed. The contact load layer is identified as the transition zone between the outer region (suspension layer) and the bedload layer. First, the physical aspects of momentum transfer are discussed and the contact layer is defined. Further, following Deigaard (1993) a new formulation of the skin friction being a combination of turbulence and the collisions between the grains, based on the diffusion concept, is postulated. Making use of the proposed solution procedure, the new system of equations is employed to compute time-dependent sediment concentration and velocity, wave-period-average concentration and transport rate (net and average in half period), together with the determination of two calibration coefficients, basically unknown in Deigaard's (1993) approach. The bedload model of Kaczmarek et al. (published simultaneously) provides the boundary conditions for the solution of the contact load layer. The comparisons between the model results and available laboratory data yield satisfactory conformity. Significant discrepancies between the model results and experimental data are found at higher levels above bed. They are most probably linked to convective events in flow reversal.

1. Introduction

It is well known that hydrodynamic processes in the wave and current bottom boundary layer are highly non-linear, see e.g. Soulsby et al. (1993) and Nielsen (1992). However, non-linearity is even more pronounced in relation to sediment transport processes, due to the additional constraints of the threshold condition for sediment motion and of the non-linear relationship between the bed shear stress and the sediment pick-up rate. Recently, sufficiently detailed near-bed velocity and sediment concentration data, e.g. Ribberink & Al-Salem (1994, 1995), have become available to test not only the overall predictions of net ratio of sediment transport made by different modelling schemes but also, very importantly, the accuracy with which these schemes represent detailed boundary layer processes in reversing oscillatory flows.

Flat beds of loose sand under waves, as well as under steady flow may offer considerably more resistance to the flow than sand paper with the same grain size. This is a consequence of the momentum transfer by moving sand from the flow to the bed. It is, however, difficult to estimate this momentum transfer and the number of related data is greatly limited. Therefore, a generally accepted method for a continuous description of processes with nonmovable bed, through to the formation of a sheet flow layer, and a suspended load, is still not well established.

Recently, Davies et al. (1997) have shown the comparisons which have been made between model predictions and measurements of both time-dependent sediment concentration, and also wave-averaged horizontal velocity and concentration. The predictions of four sediment transport models were compared with detailed laboratory data sets obtained in the bottom boundary layer beneath regular waves, asymmetric waves, and regular waves superimposed co-linearly on a steady current. They showed that our present incomplete understanding of momentum transfer and of the associated sediment pick-up, in reversing oscillatory flows imposes potentially severe limitations on existing predictive methods. First, none of the four models provided a good detailed description of the time-dependent suspended sediment concentration, due mainly to the inability of conventional turbulent diffusion schemes to represent the entrainment of sediment into suspension by convective events at flow reversal. Second, the four models discussed by Davies et al. (1997) were primarily models of sediment in suspension, and did not include physical processes which occur in the high concentration, sheet flow layer. Hence, the consistency of these approaches in terms of the choice of a matching level between the bedload and suspended load layers is highly questionable.

To resolve this matching problem, a clear physical description is needed for the processes in the layer between immobile bed and elevations where all sediment moves in suspension.

An attempt to shed light on near-bed phenomena and interactions with emphasis on sediment transport as bedload was made by Kaczmarek et al. (published simultaneously) who proposed that near-bed sediment dynamics be modelled in two regions, i.e. a lower collision-dominated granular-fluid region and an upper turbulent – fluid shear region with continuous profiles of stress and velocity connecting both regions. Comparison of model results with a range of experimental data has suggested that the model is capable of reproducing the hydrodynamic drag and sediment bedload transport quantities (thickness and rate) on flat beds of sediment for both low and high wave conditions. Hence, two types of indirect experimental evidence of the hydraulic roughness, i.e. measured bedload quantities over flat sand beds under waves and effective bed shear stresses corresponding to energy dissipation measurements are not necessarily conflicting, as indicated by Nielsen (1992).

The aspect of asymmetric and irregular wave effects on bedload has been included in the model proposed by Kaczmarek & Ostrowski (1996), which was tested – inter alia – against IBW PAN laboratory data.

Model results of Kaczmarek et al. (published simultaneously) do not, however, take into account the effect of suspended sediment on total sediment transport near the bed. The major purpose of the present study is to include this effect. It is assumed that sediment conditions are such that bed forms do not occur hence the bed can be considered flat.

The present paper is focused on the transition region (called contact layer) between the outer region (suspension layer) and the bedload layer in a three-layer sediment transport model. First, the physical aspects of momentum transfer are discussed and the contact layer is defined. Further, following Deigaard (1993) a new formulation of the skin friction, being a combination of turbulence and collision between the grains, is proposed. The proposed description of skin friction is based on the diffusion concept. Adopting the proposed solution procedure, the new system of equations is employed to compute time-dependent sediment concentration and velocity, wave-period-average concentration and transport rate (net and average in half period) in the contact load layer. In general, the computed net sediment transport in the contact layer under asymmetric waves, together with the bedload net sediment transport determined using the model of Kaczmarek et al. (published simultaneously), determines the net sediment transport in the near-bed zone only. When the sediment transport is dominated by near-bed transport the calculated values can be considered as the total net sediment transport.

The present study involves the comparison of model results with a number of data sets, including those of Zyserman & Fredsøe (1994) for reference concentration; flume data of Sumer et al. (1996) for the sheet flow layer thickness, averaged over half a wave period; sediment transport measurements of Sawamoto & Yamashita and Horikawa et al., as reported by Nielsen (1992), small scale laboratory tests carried out at IBW PAN, Gdańsk, Poland, by the authors; and, finally, oscillatory tunnel data of Ribberink and Al-Salem, as reported by Van Rijn (1993). Further, comparison is made between the model results and measurements of time-dependent and wave-averaged sediment concentration, as well as vertically-integrated net sediment transport rate, obtained in the bottom boundary layer beneath sinusoidal and asymmetric waves in the Large Oscillatory Water Tunnel at Delft Hydraulics by Ribberink & Al-Salem (1994, 1995). In all analysed cases the agreement is found to be quite satisfactory.

2. Momentum Transfer from Oscillatory Flow to Sea Bed

2.1. Formulation of the Problem

A typical vertical distribution of velocity on a rough bed is supposed to be characterised by a sub-bottom flow and main or outer flow, as shown in Fig. 1. The

figure provides an explanatory drawing with velocities and concentrations. The collision-dominated granular-fluid region stretches below the nominal static bed while the wall-bounded turbulent fluid region extends above it. The outer region of pure suspension is characterised by a very small concentration, where the process of sediment distribution may be considered as a convective and (or) diffusive process. In contrast, the granular-fluid region below the nominal bed is characterised by very high concentrations, where the intergranular resistance is predominant.

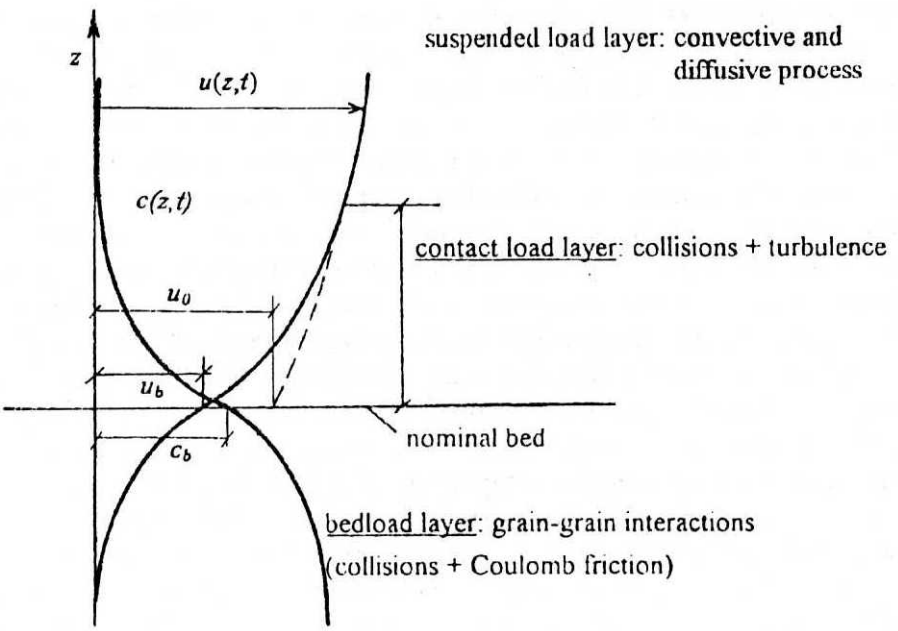

Fig. 1. Definition sketch

Since both water and grains are assumed to move in both regions, there must be a certain transition zone between these two regions, in which the velocity and stress profiles merge and preserve continuity of shape. The transition zone, called a contact load layer, is a central topic of the present study. The velocity profile in the contact load layer is assumed to be continuous. Its intersection with nominal seabed is the apparent slip velocity ub which can be identified as a characteristic velocity of sediment moving in the form of bedload. The downward extension of the velocity distribution in the outer zone of the main flow yields a fictitious slip velocity u_0 of the fluid at the nominal static bed level. Clearly, the fluid velocity u_0 is greater than the sediment velocity u_b.

The above three-layer system of momentum exchange has recently been observed in the measurements of concentrations carried out by Ribberink & Al-Salem (1995).

2.2. Physical Bases

It is traditionally assumed, see for instance Wilson (1987), that the contact load layer consists of several layers of grains in motion, and in these layers the applied shear stress τ is resisted by the sum of a granular component τ_s and a fluid component τ_f. As demonstrated by Bagnold (1956), τ_s is associated with the intergranular stresses due to particle collisions. The shear layer extends down to a certain level (say nominal bed) at which the intergranular resistance τ_s equals the applied shear stress τ. Further down towards the non-moving bed the intergranular resistance is predominant and it can be assumed that the particle interactions in the bedload layer produce two distinctive types of behaviour. The particle collisions give rise to viscous-type stresses, while further down towards the non-moving bed, Coulomb friction between particles (which remain in contact with each other) give rise to plastic-type stresses.

Because the intergranular resistance is predominant in the bedload layer, it is proposed that the weight of moving sediment is transferred to the grain skeleton in the non-moving bed.

In contrast, the sediment in the contact load layer is transported partially as bedload and partially as suspended load. This means that the sediment is carried by both the dispersive stresses and by the fluid. When the suspended sediment is carried by the fluid, its weight causes an increase in the pressure above the hydrostatic. Hence, it can not be assumed that the stress transferred to the bedload layer from the contact load layer corresponds exactly to the weight of the load. This was illustrated by Deigaard (1993) who considered a grain jumping in fluid.

Grain-grain-water interactions in the contact load layer are assumed to produce three distinctive types of behaviour. The random motion of the sediment grains, which is the basis for the diffusion process, is caused by a combination of turbulence and the collisions between the grains in the contact load layer. These two effects give rise to skin friction τ'. Aside from the skin friction, a particle exposed to a turbulent flow will additionally feel a drag due to a pressure difference on the up- and downstream sides of the grain because of flow separation. Thus, the residual part of the total shear stress $\tau - \tau'$ is carried as a drag on the moving bed particles. This drag gives rise to convective sediment exchange rather than turbulent diffusion.

The above shows that the two layers, e.g. bedload and contact load, differ considerably in proceeding momentum exchange. Hence, the interface between them, i.e. the level at which the intergranular resistance equals the applied total shear stress, can be expected as a very distinct one. This is supported by the recent

measurements of concentration carried out by Ribberink & Al-Salem (1995). The detailed measurements of concentration showed the three-layer system with a lower and upper sheet flow layer and a suspension layer. The lower and upper sheet flow layer can be identified as bedload and contact load layers, respectively. Sediment was picked up from the lower sheet flow layer at the two phases of maximum velocity during the wave cycle, resulting in two concentration dips in the lower sheet flow layer and two concentration peaks in the upper sheet flow layer.

2.3. Solution Procedure

It is next proposed that the downward extension of the velocity distribution from the suspension layer to the bedload layer is described by the logarithmic distribution and is controlled by effective bed roughness k_e. The logarithmic velocity profile extrapolated from the suspension region is positioned at $z_0 = k_e/30$, the height where the velocity profile approaches zero. Further, the flow at the top of the contact load layer is assumed to be unaffected by the transition phenomena.

These assumptions enable the problem of near-bed sediment motion to be solved within the two steps, schematically shown in Fig. 2. In the first step, the problem is reduced to bedload transport (Fig. 2a) the solution of which was proposed in a series of papers by Kaczmarek et al. (1994), Kaczmarek et al. (1995), Kaczmarek & Ostrowski (1996) and recently by Kaczmarek et al. (published simultaneously), who used a theoretical approach based on grain-grain interaction ideas in analogy to the flow of dry, cohesionless materials. The iterative procedure was employed to match the velocity and shear stress profiles in both regions (Fig. 2a) using a theoretical bed level for the outer wave-induced flow of δ_{sx}, which was taken as an arbitrary fraction of the thickness of the moving, collision-dominated bed layer δ_n.

It is proposed that the movement of sediment inside the contact load layer be solved in the second step (Fig. 2b). In this case the problem is focused on finding skin effective roughness k_e' with determination of thickness δ_c of the contact load layer. As a boundary condition it is proposed to use the instantaneous (during the wave period) sediment velocity $u_b(t)$ and concentration c_b (assumed to be constant and equal to 0.32) at the top of the bedload layer, found from the bedload model with $\delta_{sx}/\delta_n = 0.50$.

3. Computational Background

3.1. Skin Friction Concept

Following Fernández Luque's, after Fredsøe & Deigaard (1992), and Engelund & Fredsøe's (1976) ideas, the momentum transfer in the contact load layer can be

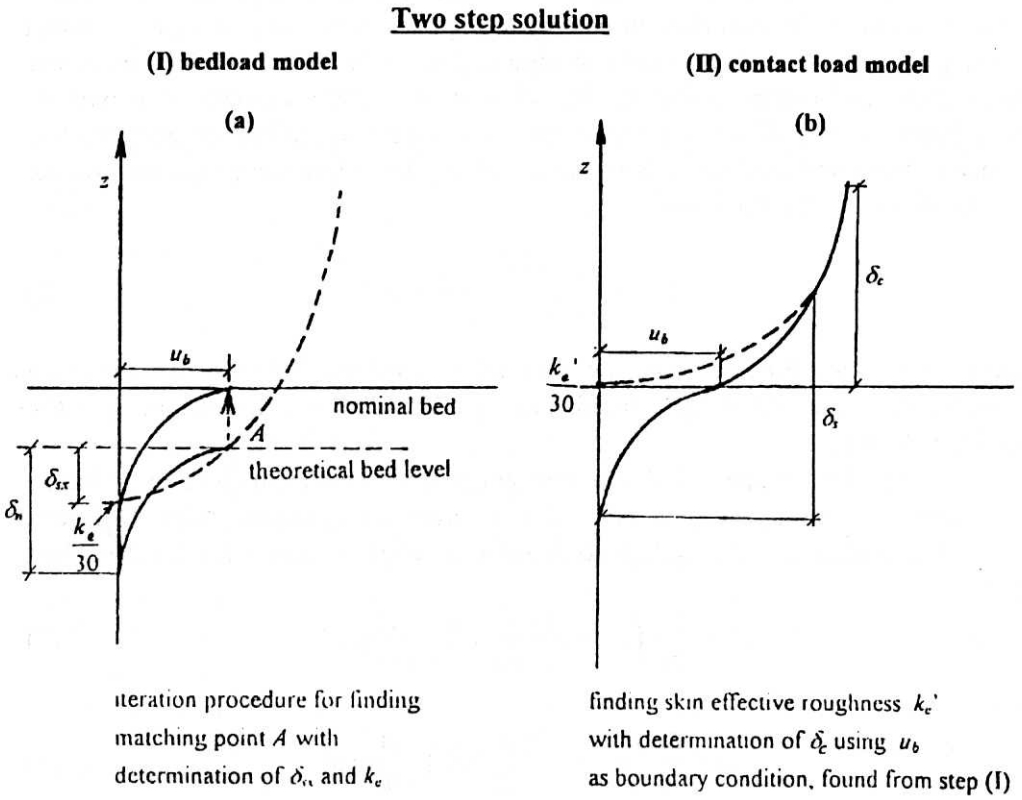

Fig. 2. Solution procedure

described by the equation:

$$\tau = \overbrace{\tau_f + \tau_s}^{\tau'} + nF_D \tag{1}$$

where F_D is the average drag on a single moving particle, while n is the number of moving particles per unit area.

It is assumed that the moving particles in the contact load layer reduce the fluid shear stress τ_f by exerting an average reaction force on the surrounding fluid. This reduction, however, is not as drastic as it is inside the bedload layer, where the intergranular resistance is predominant. Further, it is proposed that the velocity gradient inside the contact load layer is affected by the presence of sediment.

A new formulation for skin friction, which is considered as a combination of turbulence and collision between the grains, is proposed. A new model of sheet flow is developed, incorporating the diffusion concept presented by Deigaard (1993).

Each collision invoves displacement of the particles. The displacement is due to the movement of the particles on passing along each other, which is proportional to the grain size. The second contribution is due to the vertical velocities of the grains produced during collision. The change of vertical velocity of a particle immediately after collision is proportional to the velocity difference between two particles. The combined vertical displacement Δ_z, including the two contributions is to be given by the equation

$$\Delta z = \alpha \frac{du}{dz} \frac{2d^2}{3w_s} \frac{s + c_m}{c_d} + \beta d \tag{2}$$

where α and β are the coefficients, s – the relative sediment density, d – the grain diameter, c_m – the added mass coefficient, c_d – the drag coefficient and w_s – the settling velocity.

The vertical displacement of sediment grains due to collision gives an exchange of sediment in the term of a vertical concentration gradient. After Deigaard (1993), this exchange – by analogy to the mixing length theory – can be described in terms:

$$\Delta z d \frac{du}{dz} \left(c^2 - \frac{\Delta z}{2} \frac{d}{dz}(c^2) \right) \frac{A}{vol^2} vol \tag{3}$$

and

$$\Delta z d \frac{du}{dz} \left(c^2 + \frac{\Delta z}{2} \frac{d}{dz}(c^2) \right) \frac{A}{vol^2} vol \tag{4}$$

at level z for upward and downward fluxes, respectively, gives a net upward flux of

$$-3\Delta z^2 \frac{du}{dz} c \frac{dc}{dz} \tag{5}$$

The number of particles per unit volume is c/vol, where vol is the volume of a particle. A is the cross sectional area of a particle.

In addition to collisions exchange, sediment is exchanged during turbulence. The turbulence is simply described by the mixing length theory, giving

$$-l \frac{du}{dz} \frac{dc}{dz} \tag{6}$$

where l is the mixing length $l = 0.4z$.

Collisions will also cause vertical exchange of horizontal momentum. Each grain has a momentum of $\rho(s + c_m) vol\, u$, and by a derivation similar to Eqs. (3) and (4) the momentum exchange is found to be

$$2\Delta z \frac{du}{dz} c^2 \frac{dA}{vol^2} \frac{\Delta z}{2} \frac{du}{dz} vol\,(s + c_m)\rho = \rho \frac{3}{2} \Delta z^2 c^2 (s + c_m) \left(\frac{du}{dz} \right)^2 \tag{7}$$

The mixing length theory gives an exchange of flow equal to:

$$\rho l^2 \left(\frac{du}{dz}\right)^2 \tag{8}$$

By assuming that the settling of sediment keeps in balance the vertical exchange, and that the momentum exchange balances the shear stress, Deigaard (1993) proposed two coupled differential equations to determine the mean concentration profile and the velocity profile:

$$\left[\frac{3}{2}\left(\alpha\frac{d}{w_s}\frac{du}{dz}\frac{2}{3}\frac{s+c_m}{c_d}+\beta\right)^2 d^2c^2(s+c_m)+l^2\right]\left(\frac{du}{dz}\right)^2 = u_f'^2 \tag{9}$$

$$\left[3\left(\alpha\frac{d}{w_s}\frac{du}{dz}\frac{2}{3}\frac{s+c_m}{c_d}+\beta\right)^2 d^2\frac{du}{dz}c+l^2\frac{du}{dz}\right]\frac{dc}{dz} = -w_s c \tag{10}$$

In general, two coefficients α and β have to be determined, e.g. by calibration. For simplicity, equal values of α and β have been assumed in further considerations. It was assumed that $(s + c_m) = 3.0$ and $c_d = 1.0$. The boundary conditions for the above equations are that the sediment velocity u and concentration c are given at a certain level.

In the preliminary calculations, a tentative value of the sediment velocity $u_b = 0.14$ m/s was taken at the level $z = 2.5d/30$ while the sediment concentration at this level was assumed to be $c_b = 0.32$ (in conformity with the bedload model). The calculations were made for two sets of the coefficients α and β, i.e. for $\alpha = \beta = 0.053$ and $\alpha = \beta = 0.5$.

Fig. 3 shows the velocity profiles with linear and logarithmic z axes, and concentration profiles. It can be seen that the velocity profile attains a logarithmic shape at a distance from the bed. The roughness corresponding to this logarithmic profile depends on the value of $\alpha = \beta$. For the case of $\alpha = \beta = 0.053$ the roughness equals 0.000525 m while for $\alpha = \beta = 0.5$ the roughness amounts to 0.00173 m.

3.2. Reduction of Model Parameters

According to the discussion in Section 2.2 it is still not clear how to evaluate the drag due to moving sand particles. It is possible, however, to overcome these difficulties by making an additional assumption that the sediment velocity distribution at the contact load layer is controlled by effective skin roughness k_e' and that the sediment velocity profile attains a logarithmic shape at a certain distance from the nominal bed. By means of the above, sediment motion in the contact load layer is determined by Eqs. (9) and (10) and the following relationship:

$$\tau' = \tau - nF_d = \rho u_f'^2 \tag{11}$$

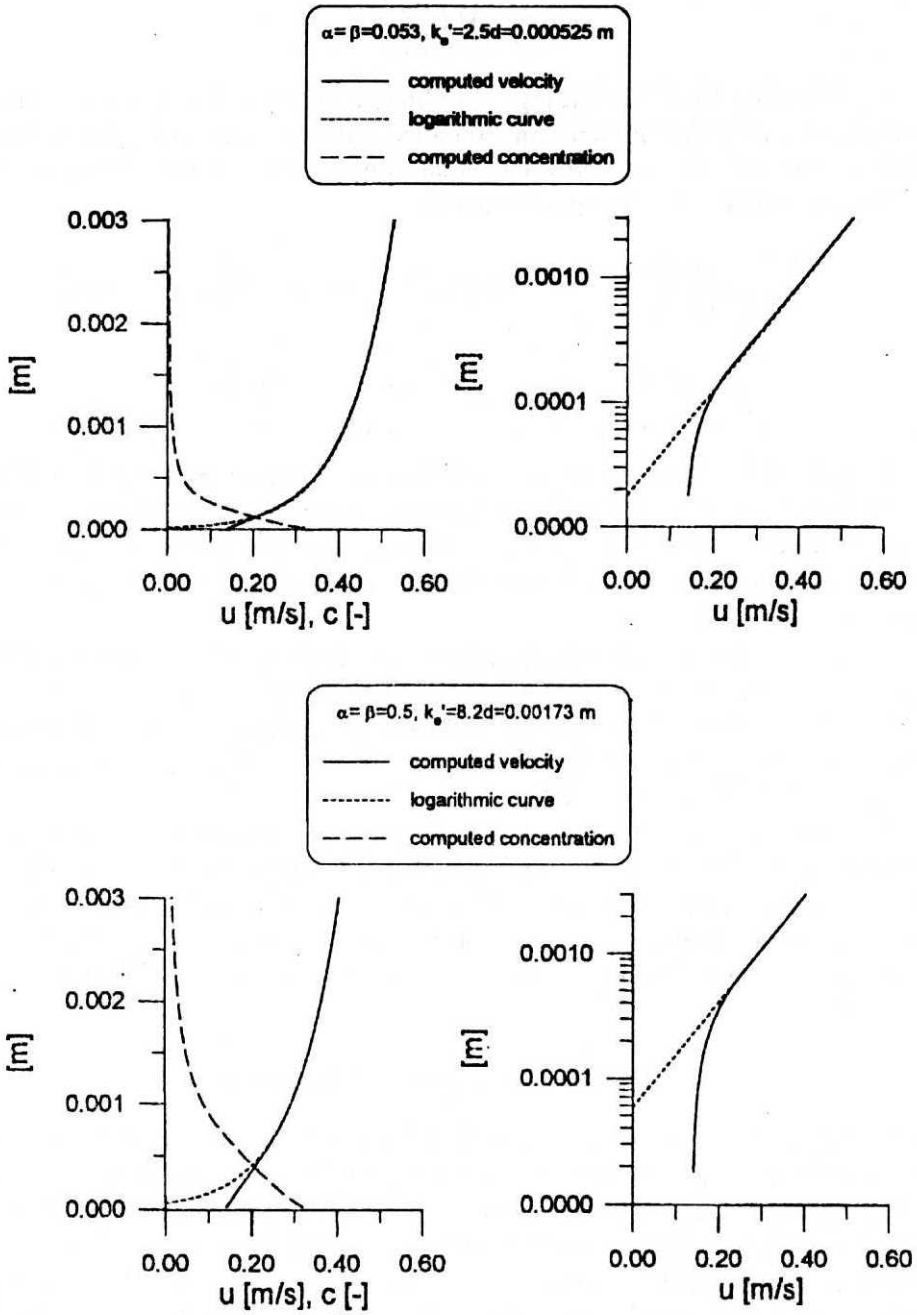

Fig. 3. Preliminary results for $u'_f = 0.041$ m/s, $u_b = 0.14$ m/s and $d = 0.21$ mm

in which u'_f is the skin friction velocity, proposed to be found using Fredsøe's (1984) differential equation for the variation of z_1:

$$\frac{dz_1}{d(\omega t)} = \frac{30\kappa^2 U(\omega t)}{k_e \omega e^{z_1}(z_1 - 1) + 1} - \frac{z_1(e^{z_1} - z_1 - 1)}{e^{z_1}(z_1 - 1) + 1} \frac{1}{U} \frac{dU}{d(\omega t)} \tag{12}$$

As a result, the function $z_1(t)$ is obtained and the temporal distributions of the boundary layer thickness $\delta(t)$ and the skin friction velocity $u'_f(t)$ are given by the following equations, respectively:

$$\delta = \frac{k'_e}{30}(z^{z_1} - 1) \tag{13}$$

$$z_1 = \frac{U\kappa}{u'_f} \tag{14}$$

in which U is the free stream velocity.

It should be noted that the free stream velocity $U(\omega t)$ can be described as linear or non-linear, thus Fredsøe's (1984) model can be adapted to non-linear (asymmetric) wave motion, as done by Kaczmarek & Ostrowski (1996).

The solution of Eq. (12) yields the values of $u'_f(t)$ if k'_e is specified as a fixed constant value. Following Nielsen (1992) a value of $2.5d$ was adopted for the effective skin roughness k'_e of the moveable flat bed.

Knowing the instantaneous (during the wave period) skin shear stress $\rho u'^2_f(t)$ it is possible to calculate sediment concentration $c(z, t)$ and velocity $u(z, t)$ in the contact load layer using Eqs. (9) and (10) with the boundary conditions $u_b(t)$ and c_b given at $z = k'_e/30$ from the bedload solution with $\delta_{sx}/\delta_n = 0.50$. The proposed solution depends on the coefficients α and β ($\alpha = \beta$). Making use of the fact that the velocity attains a logarithmic shape at a certain distance from the bed and that the roughness corresponding to this logarithmic profile depends on α, an iterative procedure is employed to find $\alpha = \beta$. The sought value of $\alpha = \beta$ which provides the match of velocity profile yielded by Eqs. (9) and (10) with the logarithmic profile described by the skin friction parameters (k'_e and u'_f). The match is found at the moment corresponding to the maximum skin shear stress.

The solution is restricted by a number of simplifying assumptions. Therefore, the proper determination of the layer thickness δ_c identified as the solution validity limit, plays a very important role. The selection of criterion for d_c can be based on the degree of fit of experimental data comprising sediment concentrations and transport rate within the contact load layer. In the next section, two values for the upper limit of the contact load layer are tested against laboratory data, namely $\delta_1/4$ and $\delta_1/2$, where δ_1 is the thickness of the bed boundary layer $\delta(t)$ calculated from Fredsøe's (1984) model at the moment corresponding to maximum free stream velocity. The value $\delta_1/2$ can be identified as the conventional bottom

boundary layer thickness while $\delta_1/4$ denotes the upper limit of the region where the logarithmic velocity profile is observed.

Finally, it is worthwhile noting that the turbulence damping by suspended particles is represented in the model by the following relationships:

$$\varepsilon = \beta_1 \varepsilon = \beta_1 \kappa u_f z \tag{15}$$

$$\varepsilon_s = \kappa z(\beta_1 u_f) = \kappa z u'_f \tag{16}$$

in which ε_s is the mixing coefficient for solid material, κ is von Karman's constant (=0.4) and β_1 is a factor which, according to Deigaard, after Fredsøe & Deigaard (1992), is always smaller than the turbulent momentum exchange coefficient ε, with difference proportional to w_s/u_f.

4. Results of Computations Versus Laboratory Data

4.1. Reference Concentration and Sheet Flow Layer Thickness

The model has been run for two sets of water depth and wave period ($h = 10$ m, $T = 8.39$ s and $h = 5$ m, $T = 3.6$ s) and for the grain diameter $d = 0.2$ mm. In addition, the first set of depth and period values has been run for grain diameter $d = 0.7$ mm. The wave height has been changed in each run so that a wide range of sediment transport intensities has been analysed. The model results for concentration at $z = 1.5d$ have been compared with the experimental data of Guy et al., as interpreted by Zyserman & Fredsøe (1994). The comparison, shown in Fig. 4, affords quite good agreement.

The same sets of computational parameters have been used in the modelling of the sheet flow layer thickness δ_s. The upper limit of this layer has been interpreted as the level at which the model result for velocity at the moment corresponding to the maximum skin shear stress attains the logarithmic velocity distribution with an accuracy of 99% (cf. velocity profiles in Fig. 3). The distance between the above defined level and $z = k'_e/30$, summed up with the bedload layer thickness by Kaczmarek et al. (published simultaneously), yields the sheet flow layer thickness and is shown in Fig. 5 as a function of dimensionless maximum skin shear stress, i.e. $\theta'_{\max} = u^2_{f'\max}/[(s-1)gd]$. It can be seen that the sheet flow layer thickness, even in very severe storm conditions, does not exceed 20 grain diameters. Good conformity between theoretical findings for the sheet flow layer thickness from the present model and the experimental data of Sumer et al. (1996) has also been found, see Fig. 6.

4.2. Time-Dependent and Mean Concentration

The data used in the present comparisons were obtained by Ribberink & Al-Salem (1994, 1995) for regular symmetrical and asymmetrical waves. The experiments

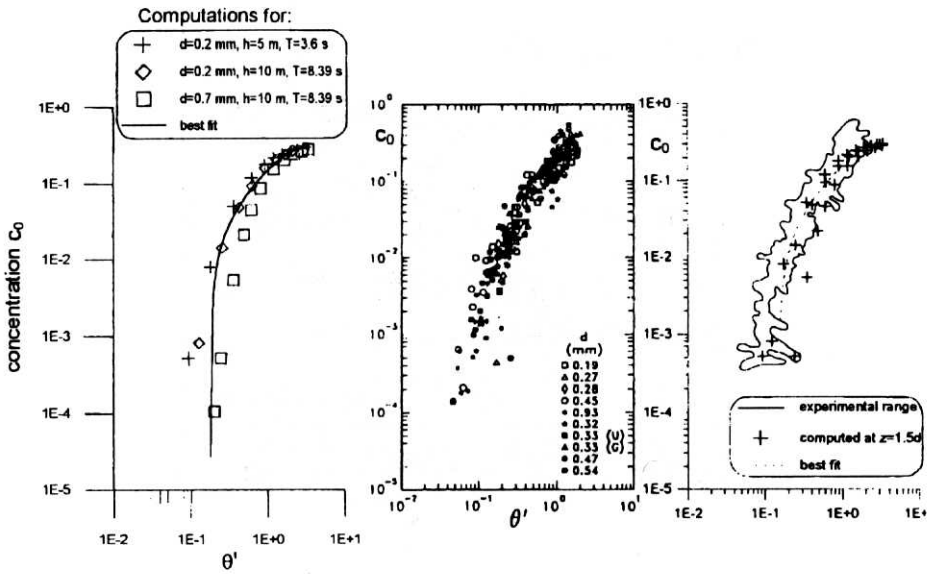

Fig. 4. Bed concentration c_0: model results vs. experimental data by Guy et al. as interpreted by Zyserman & Fredsøe (1994)

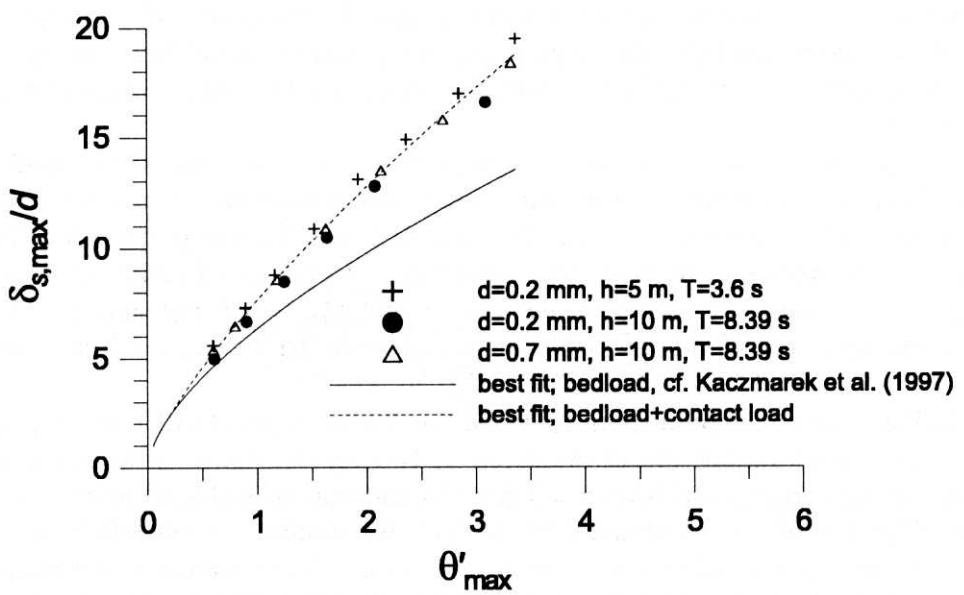

Fig. 5. Theoretical sheet flow layer thickness

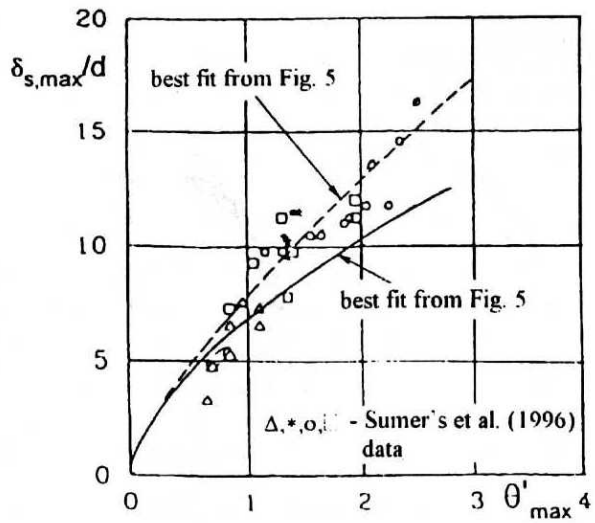

Fig. 6. Sheet flow layer thickness: model results vs. experimental data by Sumer et al. (1996)

were carried out in the Large Oscillating Water Tunnel (LOFT) at Delft Hydraulics. All the data were obtained above plane sand beds, corresponding to very vigorous conditions in nature, with median grain diameter $d = d_{50} = 0.21$ mm. Suspended sediment concentrations were measured principally with an optical concentration meter (OPCON) while concentrations in the sheet flow layer were measured using a conductivity concentration meter (CCM), see Al-Salem (1993) for details.

In the comparisons discussed below the aim has been to compare the model predictions with emphasis on time-variation in sediment concentration $c(z,t)$ at different heights (z) above the bed. The data sets used for this purpose are the series "C" of Ribberink & Al-Salem's experiments: Conditions 1 and 2 for asymmetric waves, with $U_{rms} = 0.6$ m/s, $T = 6.5$ s and $U_{rms} = 0.6$ m/s and $T = 9.1$ s, respectively, and Condition 3 for sinusoidal wave, with $U_{rms} = 1.2$ m/s and $T = 7.2$ s.

In Fig. 7 the model predictions for Condition 2 are compared with time-varying sediment concentrations $c(z,t)$ measured at two representative ordinates with respect to the original bed level $z = 0$ (i.e. the undisturbed bed level prior to the start of the experiment, identified as $z = k'_e/30$ in the model). The curve for $z = -1$ mm has been produced (for the time sectors in which the sediment movement occurs) using the bedload model of Kaczmarek et al. (published simultaneously) while for $z = +1$ mm the concentration has been computed by the present contact load model. At both levels the prediction shows satisfactory agreement with the

data. The concentration at $z = 0$ is assumed to be $c_b = 0.32 = 848$ g/l (with grain density of 2650 kg/m^3),

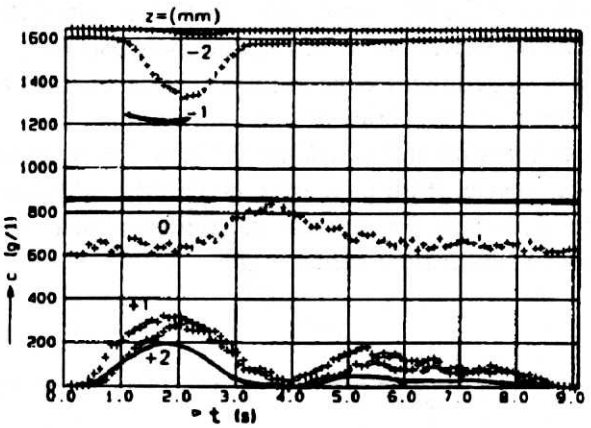

Fig. 7. Time-dependent concentrations: model results for $z = -1, 0, +1$ mm (solid lines) vs. measurements of Condition 2 (symbols), data after Al-Salem (1993)

The agreement between the model and experimental time-dependent concentrations has also been achieved for Condition 1. Here, the comparison shown in Fig. 8 is made for $z = +1$ mm only. The model bedload concentration for Condition 1 was presented by Kaczmarek et al. (published simultaneously).

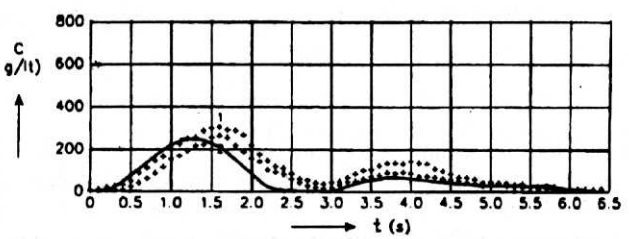

Fig. 8. Time-dependent concentrations: model results for $z = +1$ mm (solid line) vs. measurements of Condition 1 (symbols), data after Ribberink & Al-Salem (1995)

Next, an attempt has been made to model the concentration using the present contact load layer model at a higher level, namely at $z = 1$ cm, for Condition 2. The result is shown in Fig. 9. It can be seen that at higher levels (0.5–1.8 cm) the

measured time series of $c(z,t)$ develops a more complicated structure, and conformity of phase between the model and the data is lost. Furthermore, the model clearly overestimates the experimental values at the wave crests and underestimates – along the rest of the wave phase. The reason for the failure of the model to predict the phase angle of the time-dependent concentration is the appearance, at around the time of flow reversal in the free stream between wave crest and trough, of an additional peak in sediment concentration. Near the bed ($z = 0.5$ cm) this peak is very small and the time series of concentration is dominated by the main diffusion peak associated with the maximum velocity, hence maximum bed shear stress, during the wave cycle. With increasing height, the additional peak grows in relative importance, becoming larger than the diffusion peak at $z = 1.8$ cm and dominating the concentration time series.

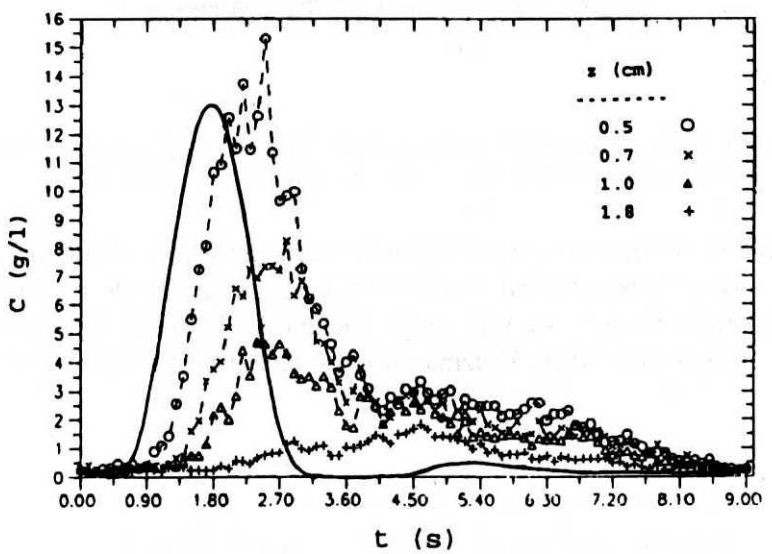

Fig. 9. Time-dependent suspended sediment concentrations: model results for $z = +1$ cm (solid line) vs. measurements of Condition 2 (symbols), data after Al-Salem (1993)

The importance of this additional concentration peak, identified by Davies et al. (1997) as a convection peak, is demonstrated in experiments for asymmetric waves, by Ribberink & Al-Salem (1994, 1995) who found that unsteadiness in u and c produced an "onshore" net transport of sediment close to bed, and an "offshore" transport above this in the outer suspension layer.

Hence, the ordinate of $\delta_1/4$ (which corresponds to $z = 0.5$ cm for Condition 2) determines the upper limit of the region where the phase agreement exists between the model and data concentrations. This value can be recommended as

the upper boundary of the contact load layer for the purpose of net sediment transport calculations.

However, despite the failure to predict the phase angle of $c(z,t)$ in the outer suspension layer, the model provides a reasonably accurate vertical profile of wave-period-averaged concentration $< c >$ up to the level of $\delta_1/2$, as shown in Figs. 10, 11 and 12 for Conditions 2, 1 and 3, respectively.

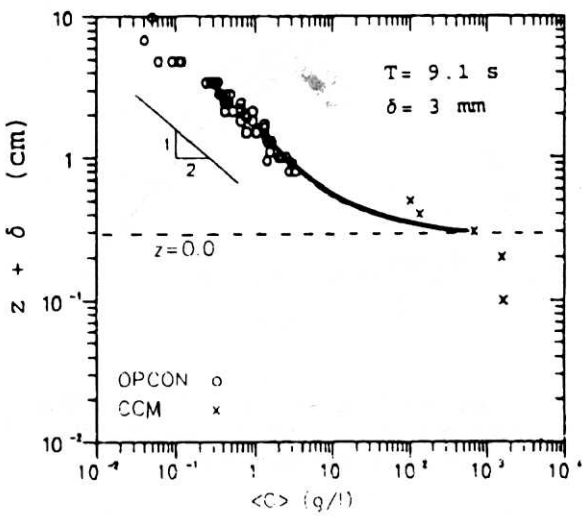

Fig. 10. Time-averaged concentration profiles: model results (solid line) vs. measurements of Condition 2 (symbols), data after Al-Salem (1993)

Further evidence of good model predictions in the context of time-averaged concentration is depicted in Fig. 13 where the model results for $z = 1$ cm are compared with experimental data of 10 wave series B and 3 series C of measurements by Ribberink & Al-Salem (1994, 1995), as well as in Fig. 14 where time-averaged vertically-integrated (up to $\delta_1/2$) concentrations (sediment load L_t) are compared with the tunnel data (series B) by Ribberink & Al-Salem, as reported by Van Rijn (1993).

Hence, the above results suggest that $\delta_1/2$ is a good measure of the upper limit of the contact load layer for calculations of time-averaged concentration and half-period sediment transport rate, in which phase shifts between concentration and velocity are not that important.

In addition, Figs. 11 and 12 show that the plots of Davies et al. (1997) work, these having compared the predictions of four 1DV boundary layer models of suspended load with differing diffusive closure schemes: one-equation turbulent kinetic energy (t.k.e.), $k - L$, mixing length; and eddy viscosity (STP) models. None of these models, as well as the present model, provide a good detailed

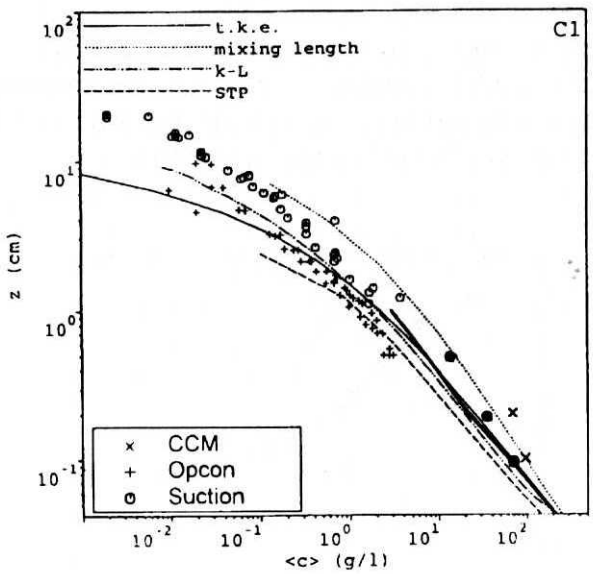

Fig. 11. Time-averaged concentration profiles: model results (thick solid line) vs. measurements of Condition 1 (symbols), Ribberink & Al-Salem data after Davies et al. (1997), and various theoretical approaches (lines)

description of the time-dependent sediment concentration in the outer suspension layer, due mainly to the inability of conventional turbulent diffusion schemes to represent the entrainment of sediment into suspension by convective events at flow reversal. On the present evidence, no clear-cut case can be made for the advantages of sophisticated turbulence closure schemes inside the contact load layer. However, the present model, together with the bedload model of Kaczmarek et al. (published simultaneously), provides a continuous description of processes from the immobile bed, through the bedload layer, the contact load layer, up to the outer suspension layer, while the models discussed by Davies et al. (1997) are aimed primarily at the prediction of the sediment distribution in the low concentration suspension layer.

4.3. Half-Period Averaged and Net Sediment Transport

The same sets of computational parameters as used for determination of the sheet flow layer thickness in Section 4.1 have been assumed as the model input in the computations of sediment transport rate averaged over half a wave period. In accordance with the discussion on the contact load layer thickness in Section 4.2, the computations comprise the layer up to $\delta_1/2$. The model results are presented

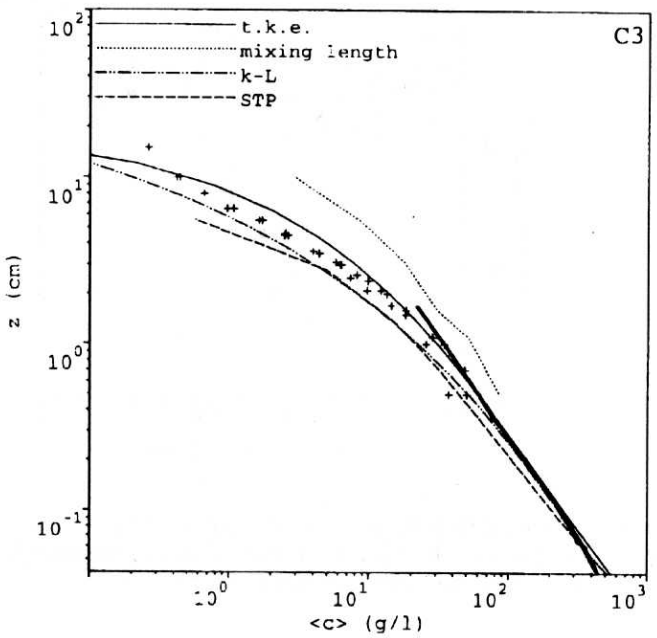

Fig. 12. Time-averaged concentration profiles: model results (thick solid line) vs. measurements of Condition 3 (symbols), Ribberink & Al-Salem data after Davies et al. (1997), and various theoretical approaches (lines)

in Fig. 15 as a function of $\theta_{2.5}$ defined by the equation:

$$\theta_{2.5} = \frac{1}{2} f_{2.5}\ \psi_1 = \frac{1}{2} f_{2.5} \frac{(a_{1m}\omega)^2}{(s-1)gd} \tag{17}$$

in which the special grain roughness friction factor $f_{2.5}$ is based on a roughness $2.5d_{50}$, where d_{50} is a median grain size, using the equation, Nielsen (1992):

$$f_{2.5} = \exp\left[5.213\left(\frac{2.5d_{50}}{a_{1m}}\right)^{0.194} - 5.977\right] \tag{18}$$

As one could expect, for low shear stresses, sediment transport consists mainly of bedload while for higher shear stresses it is dominated by suspended load. The contribution of suspended load is obviously bigger for fine sediments. It can be seen from Fig. 15 that this contribution at low shear stresses is slightly more pronounced for small wave periods while at high shear stresses, suspended load is a little larger for long period waves. The above results from bigger values of maximum shear stress and – on the other hand - smaller values of δ_1 for short

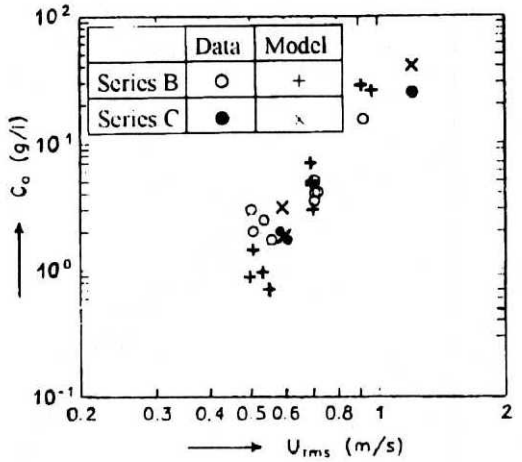

Fig. 13. Time-averaged concentrations at $z = 1$ cm: model results (+ and × for series B and C, respectively) vs. measurements (○ and • for series B and C, respectively), by Ribberink & Al-Salem (1994, 1995)

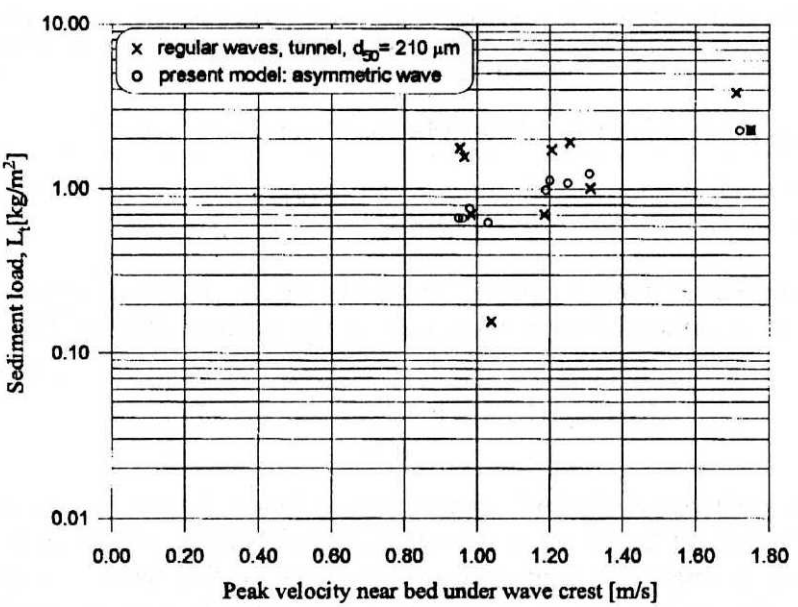

Fig. 14. Time-averaged sediment load: model results vs. measurements by Ribberink & Al-Salem, laboratory data after Van Rijn (1993)

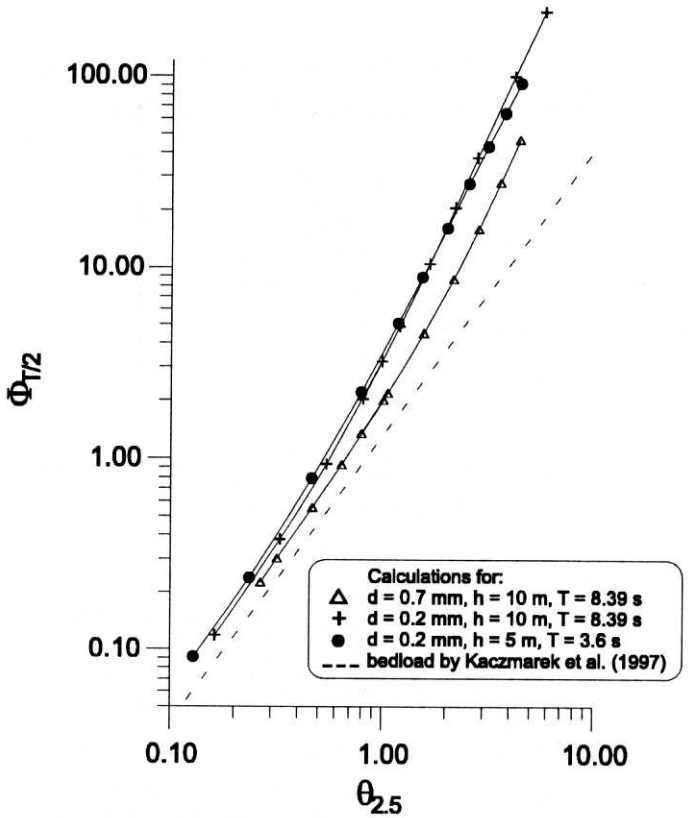

Fig. 15. Model sediment transport rate averaged over half wave period

periods. The value of δ_1 plays a more important role in the regime of suspended load, thus a grater suspended load contribution is achieved at high $\theta_{2.5}$ for long wave periods.

The model results are compared in Fig. 16 with laboratory half-period sediment transport measurements. Since no significant differences between long and short wave period results have been found, one approximation for long and short wave period, for $d = 0.2$ mm, is given in Fig. 16.

Finally, the comparison between predicted and observed net sediment transport rates for Ribberink & Al-Salem's (1994) experiments is presented in Fig. 17. Here, following the discussion in Section 4.2 on the upper validity limit for net transport determination, computations have been carried out up to the level of $z = \delta_1/4$ only. With the exception of one experiment, compliance between calculated and measured values is reasonable.

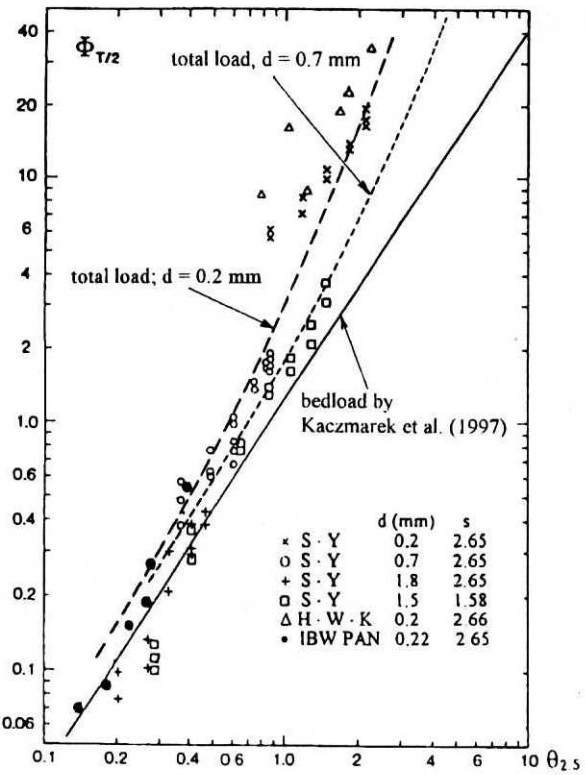

Fig. 16. Sediment transport rate averaged over half wave period: model results vs. laboratory data of Sawamoto & Yamashita and Horikawa et al., as given by Nielsen (1992), and IBW PAN laboratory data

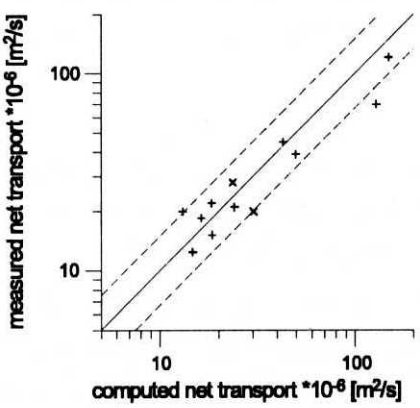

Fig. 17. Comparison between predicted and observed net sediment transport rates for 10 of Ribberink & Al-Salem's (1994) series B experiments (+) and for 2 of the series C (×), the dashed lines indicate factor 1.5

5. Conclusions

A contact load layer model, being an extension of the bedload model of Kaczmarek et al. (published simultaneously), is proposed for the calculation of sediment transport features, such as sheet flow layer thickness, sediment concentration and velocity distributions with depth in the vicinity of the bed under sinusoidal and asymmetric waves. The bedload model is a basis of the proposed approach as it provides the boundary conditions for the solution of the contact load layer which makes use of the equations proposed by Deigaard (1993). An iterative procedure has been developed to determine two calibration coefficients, basically unknown in Deigaard's (1993) approach.

The comparisons made between the model results and available laboratory data in all analysed cases yield satisfactory conformity. Significant discrepancies between the model results and the experimental data, in the context of time-dependent concentrations, are found at higher levels of the contact load layer. They are most probably linked to convective events in flow reversal. Now, there is a need to carry out further studies in order to include the description of convective terms in the present model.

6. Acknowledgements

This study contributes to the research project INDIA carried out under the EU Environment and Marine Science and Technology (MAST III) programme and is sponsored by KBN, Poland, under SPUB and programme 2 IBW PAN. The authors wish to thank Professor Brian A. O'Connor from the University of Liverpool for discussion and helpful suggestions in the preparation of the final version of this paper.

References

Al-Salem A. (1993), *Sediment transport in oscillatory boundary layers under sheet-flow conditions,* Ph.D. Thesis, Delft Hydraulics.

Bagnold R. A. (1956), The Flow of Cohesionless Grains in Fluids, *Phil. Trans. Roy. Soc.,* London, Ser. A, Vol. 249, 235–297.

Davies A. G., Ribberink J. S., Temperville A. and Zyserman J. A. (1997), Comparisons between sediment transport models and observations made in wave and current flows above plane beds, *Coastal Engineering* 31, 163–198.

Deigaard R. (1993), Modelling of sheet flow: dispersion stresses vs. the diffusion concept, *Prog. Rep. 74, Inst. Hydrodyn. and Hydraulic Eng.,* Tech. Univ. Denmark, 65–81.

Engelund F. and Fredsøe J. (1976), A sediment transport model for straight alluvial channel, *Nordic Hydrology,* Vol. 7.

Fredsøe J. (1984), Turbulent boundary layer in combined wave-current motion, *Jnl Hydraulic Eng., ASCE,* Vol. 110, No. HY8, 1103–1120.

Fredsøe J. & R. Deigaard (1992), Mechanics of coastal sediment transport, *Advanced Series on Ocean Engineering,* Vol. 3, World Scientific, Singapore.

Kaczmarek L. M., Harris J. M. and O'Connor B. A. (1994), Modelling Moveable Bed Roughness and Friction for Spectral Waves, *Proceedings of 24th International Conference on Coastal Engineering,* ASCE, 300–314.

Kaczmarek L. M., Ostrowski R. and Zeidler R. B. (1995), Boundary Layer Theory and Field Bedload, *Proc. International Conference on Coastal Research in Terms of Large Scale Experiments (Coastal Dynamics '95),* ASCE, 664–675.

Kaczmarek L. M. and Ostrowski R. (1996), Asymmetric and Irregular Wave Effects on Bedload: Theory versus Laboratory and Field Experiments, *Proc. ICCE,* ASCE, 3467–3480.

Kaczmarek L. M., O'Connor B. A. and Zeidler R. B. (published simultaneously), Bedload Transport due to Waves versus Laboratory Experiments, *Archives of Hydro-Engineering and Environmental Mechanics.*

Nielsen P. (1992), Coastal bottom boundary layers and sediment transport, *Advanced Series on Ocean Engineering,* Vol. 4, World Scientific, Singapore.

Ribberink J. S. and Al-Salem A. (1994), Sediment transport in oscillatory boundary layers in cases of rippled beds and sheet flow, *Jnl Geoph. Res.,* Vol. 99, No. C6, 12,707–12,727.

Ribberink J. S. and Al-Salem A. (1995), Sheet flow and suspension of sand in oscillatory boundary layers, *Coastal Engineering,* No. 25, 205–225.

Soulsby R. L., Hamm L., Klopman G., Myrhaug D., Simons R. R. and Thomas G. P. (1993), Wave-current interaction within and outside the bottom boundary layer, *Coastal Engineering,* No. 21, 41–69.

Sumer B. M., Kozakiewicz A., Fredsøe J. and Deigaard R. (1996), Velocity and concentration profiles in sheet-flow layer of movable bed, *Jnl Hydraulic Eng.,* Vol. 122, No. 10.

Van Rijn L. C. (1993), *Principles of sediment transport in rivers, estuaries and coastal seas,* Aqua Publications, the Netherlands.

Wilson K. C. (1987), Analysis of Bed-Load Motion at High Shear Stress, *Jnl Hydraulic Eng.,* Vol. 113, No. 1, 97–103.

Zyserman J. A. and Fredsøe J. (1994), Data analysis of bed concentration of suspended sediment, *Jnl Hydraul. Res.,* Vol. 120, No. 9, 1021–1042.